Journal of Environment and Earth Science
ISSN 2224-3216 (Paper) ISSN 2225-0948 (Online)
Vol.8, No.5, 2018

Lithostructural description and metalogeny of Alagbede gold deposit, West Central Nigeria

Ajadi, Jimoh[1*], Dada, Silas Sunday[2], Nnabo, Paulinus N.[3] and Owoeye, Beatrice Adedamola[4]

1. Kwara State University, Malete. Nigeria

2. Al-Hikmah University, Ilorin. Nigeria

3. Ebonyi State University, Abakaliki. Nigeria

4. Obafemi Awolowo University, Ile-Ife. Nigeria

*E-mail of the corresponding Author: jimoh.ajadi@kwasu.edu.ng

Tertiary Education Trust Fund (TETFUND) of Nigeria provided part of the funds for this research.

Abstract

Alagbede gold deposit located about 25km northwest of Malete in Moro Local Government Area of Kwara State, West Central Nigeria consists of gold-bearing quartz veins as stringers set in metasediments (quartzites and talc schist) overlying the migmatite gneiss basement. It is a southern extension of the northwestern end of Yauri goldfield, resulting from the development of the intercontinental Anka-Yauri-Iseyin (AYI) transcurrent fault during the Pan-African. Evidence of granitization abounds within the gneisses of the area. Structural features mapped in the area include folds, faults and joints. Discordant and concordant shear planes are partly healed with vein quartz ranging from 2-8m depth. The ongoing study indicates the preponderance of a reducing environment of sulphide association with fine-grained gold in vein quartz and schitose rocks. The general NNE to SSW trends suggest a temporal and spatial correlation with other Nigeria goldfields.

Keywords: Gold, Deposit, Metasediments, Transcurrent, Fault, Sulfide.

1. Introduction

The study area, Alagbede, lies in the west central Nigeria and bounded by latitudes 8°42'N to 8°55'N and longitudes 4°20'E to 4°35'E. The area is underlain by rocks of the basement complex of Nigeria and in fact forms the southern extension of the northwestern end of Yauri goldfield, resulting from the development of the intercontinental Anka-Yauri-Iseyin (AYI) transcurrent fault during the Pan-African. Alagbede area is located about 30km NW of Malete and is accessible through Ilorin, the Kwara State capital, via Shao – Malete – Alagbede. The Pan-African terrain that underlain the west central Nigeria falls within the Late Proterozoic – Early Phanerozoic basement separating the West African and Congo cratons (Fig. 1). It consists of an older crust with recorded Archean (ca. 2700 Ma) and Early Proterozoic (ca. 2000 Ma) ages (Grant et al., 1972) which have been widely reactivated by the Pan-African event (600± 150 Ma) (Turner, 1983; Wright et al., 1985). The Pan African event brought about regional metamorphism, a generally N–S foliation trend and the emplacement of granitoids in the region (Turner, 1983).

A continent-continent collision-type orogeny has been suggested by Wright et al. (1985) which involve an eastward dipping subduction zone where the West African Craton dips beneath the Pan-African region. The continental collision was accompanied by deformation and metamorphism around 660 Ma ago resulting in crustal thickening in the Nigerian region. Dunstan (1911) first reported on the occurrence of gold in Nigeria and by 1913 official small scale mining started. However, several authors have studied the gold mineralization and the host rocks in Nigeria e.g. Woakes and Bafor (1984) and Garba (2000, 2003). Gold mineralization is present in alluvial and eluvial placers and primary veins from several parts of supracrustal (schist) belts in the western part of Nigeria prominent of which are those found in Maru, Anka, Malele, Tsohon Birnin Gwari – Kwaga, Gurmmana, Bin Yauri, Okolom – Dogondaji and Iperindo areas (Garba 2003) (Fig. 2). All these areas are spatially related to the two fault systems in the region. The gold-bearing veins, reefs and stringers are often localized by brittle and ductile fault structures or planes of schistosity that traverse schists, quartzites, gneisses and contact aureoles of granitoid masses (Garba 2003). Due to the absence of any systematic exploration and development, the study area is presently experiencing intense artisanal workings which target both the primary gold-quartz reefs and their associated alluvial occurrences. Hence, this study focuses on detailed geologic setting, petrography and ore forming minerals distribution of the gold and associated elements in rocks of the Alagbede area.

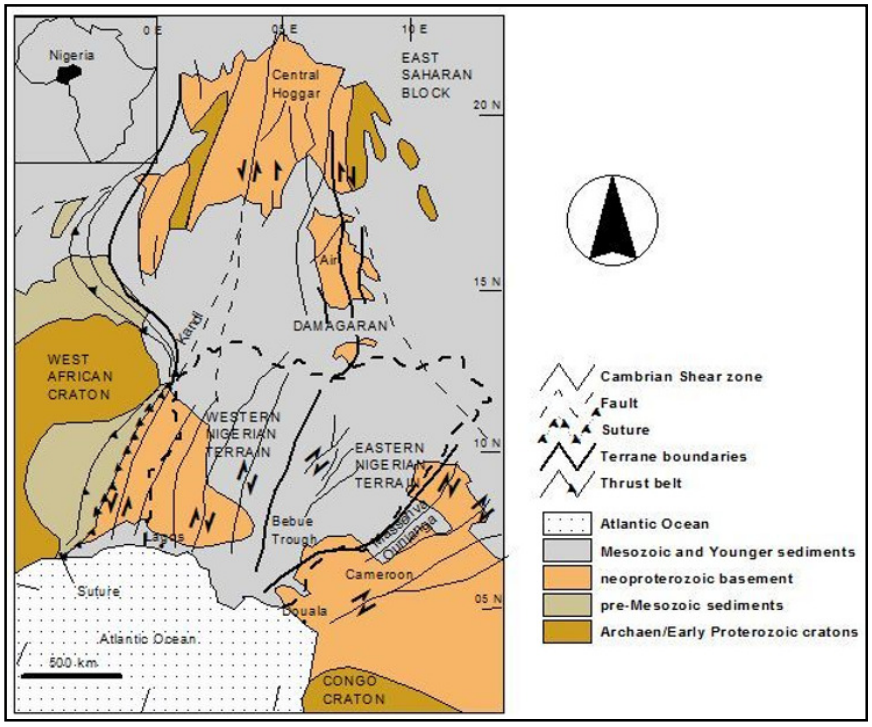


Figure 1. A generalised geological map of the Hoggar–Aır–Nigeria province within the Late Proterozoic – Early Phanerozoic basement separating the West African and Congo cratons (After Ferre et al., 2002).

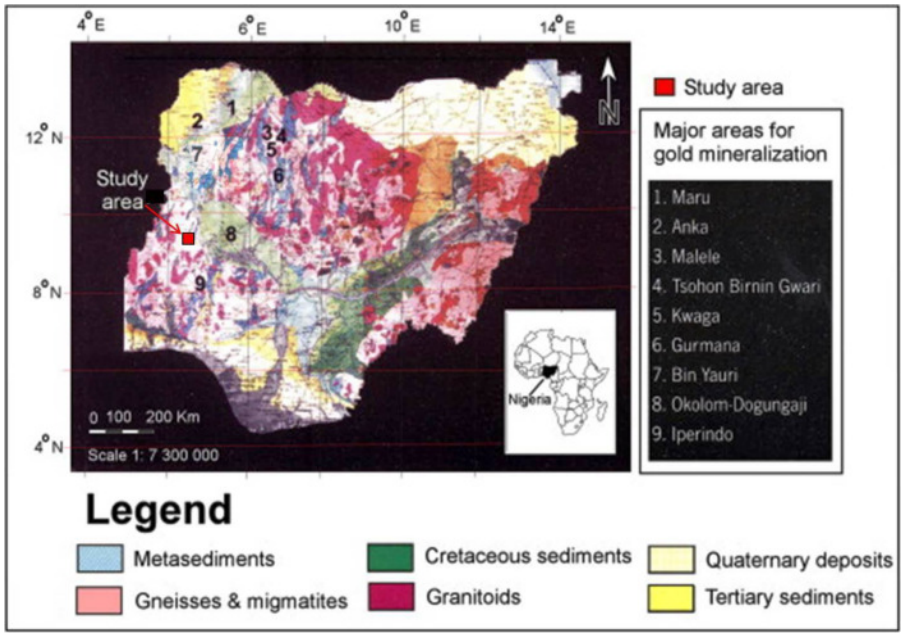


Figure 2. Geological map of Nigeria showing the major areas of gold mineralization and location of the study area (Modified after the Geological Survey of Nigeria).

2. Methodology

An initial reconnaissance survey of the area was undertaken to get acquainted with the study area while traverses were planned for ease of sampling. This was followed by a comprehensive field mapping and rock sampling of

the area to collect a total of 128 bedrock samples of the various rock units including the contact zone and associated quartz veins within the study area. The fieldwork was based on geological mapping on a scale of 1:25,000 which includes a week of reconnaissance survey which was undertaken to get acquainted with the study area and to plan traverses for ease of sampling while this was followed up with a six weeks of detailed field mapping using a combination of road and compass traversing method to access rock outcrops. The Global Positioning System (GPS) was used for precise siting of rock outcrops while the compass clinometer was used to measure trend and dips of lithologies and other structural features observed on outcrops. 30 Representative rock samples for petrographic studies were taken for thin-sectioning and petrographic studies to determine rock mineralogy under the microscope. Samples of the gold-bearing quartz veins were obtained, pulverized and analyzed for gold and sulfide composition by fire assay. The mineralized rock samples were also crushed and panned in addition to stream sediment which was also panned to determine the level of gold mineralization and grade.

3. Geological Setting and Petrography

The study area is underlain by rocks that are typical of the basement complex of Nigeria (figure 3), some of which show metamorphic imprints that are indicative of various degree of deformation they have suffered. These rocks include the migmatitic gneiss, quartzite, quartz-mica schist, talc-tremolite schist, porphyroblastic granite, porphyritic granite, coarse-grained alkali granite, medium-grained granodiorite, medium-grained alkali granite, alkali syenite, pegmatite/aplite and vein quartz.

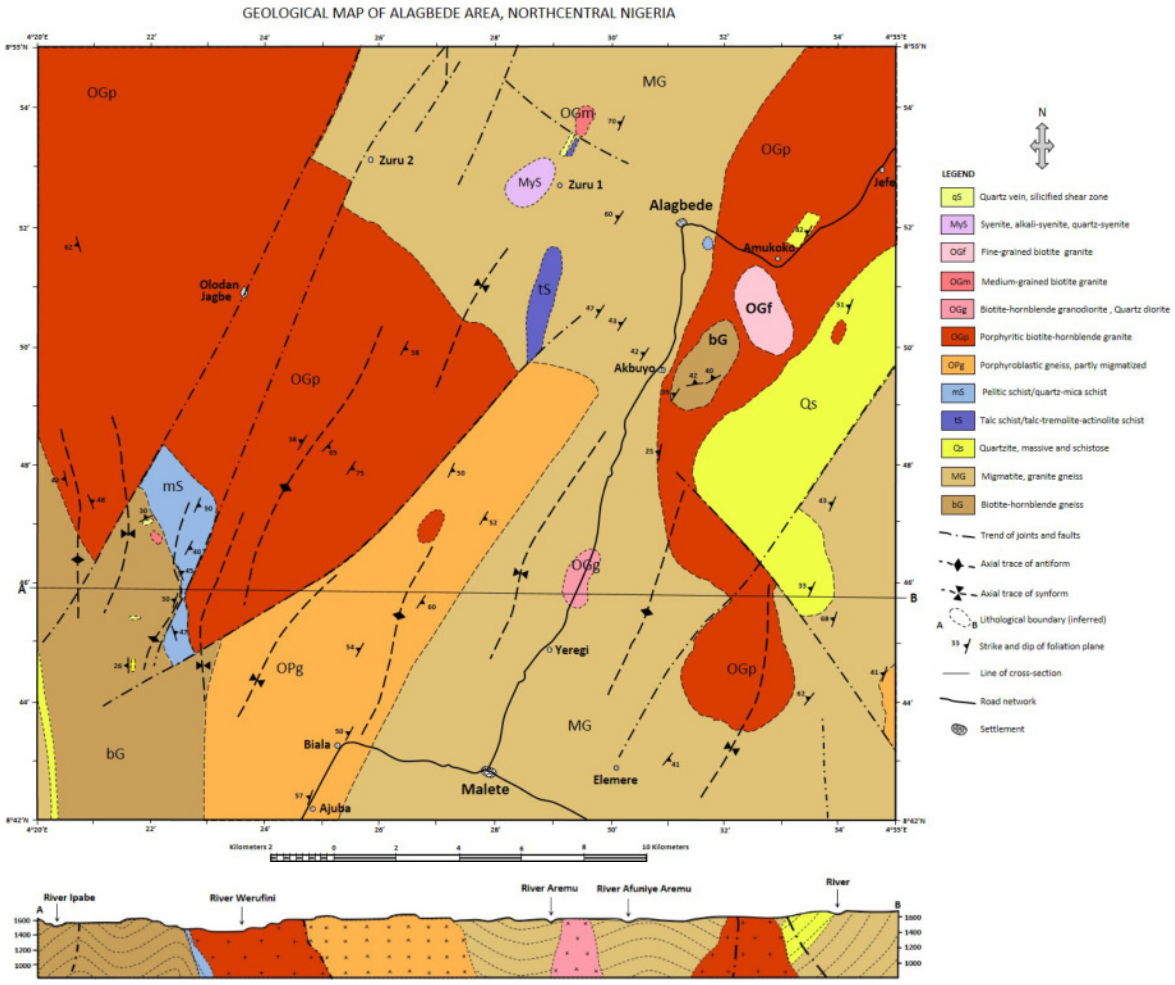


Figure 3. Geological map and cross-section of the Alagbede area showing rock distribution and structural trends.

3.1 Migmatitic Gneiss

The rock underlain about 45% of the study area and in fact constitutes the country rock hosting other rock types in the area. The rock outcrops in a variety of ways; mostly as broad low lying exposures and sometimes as low ridges and inselbergs. A number of migmatitic structures were mapped comprising of stromatic, ophthalmic and schollen types (figures 4a, 4b and 5a). The palaesome in the rock is made up of biotite gneiss while the leucosome is made up granitic gneisses, pegmatite and vein quartz. The gneisses in the study are made up of biotite gneiss, granite gneiss as well as augen gneiss and are all medium to coarse-grained in hand specimen. The occurrences of these gneisses on a single outcrop together with other granitic rocks give rise to the various migmatites mapped in the study area. In some instances the various gneissic units outcrop as discrete mappable bodies such as the fine-grained flaggy biotite gneiss outcropping between Gbara and Ejidongari villages (figure 5b) and the biotite-hornblende outcrops in the eastern and southwestern parts of the study area respectively. Under thin section (figures 6 and 7), the biotite gneisses show variable grains of minerals sizes which are closely packed and strongly foliated.

Quartz is colourless under PPL and easily distinguished by its low birefringence uniaxial positive, and absence of cleavage and alteration. Biotite is seen as large plates, brown to dark green in colour and contains inclusions of opaque minerals. The biotite crystals are elongated and define the strong foliation pattern observed. It shows pleochroism from dark brown to black and a perfect cleavage in one direction. The plagioclase in the gneisses constitutes about 10%-30% with low relief and colourless under a plane polarized light. It crystals are strongly pleochroic and they are characterized by polysynthetic (repeated) twinning; where the crystal is divided up, into narrow lamellae with alternate orientation. The migmatitic granite gneiss, under the thin section shows the following mineral assemblage: quartz (64%) + plagioclase (20%) + microcline (5%) + orthoclase (5%) + biotite (3%) + hornblende (2%) + opaque (0.8%) + accessory minerals (0.2%).

3.2 Quartzite

Quartzite bodies in the study area mostly occurs in angular blocks of rubbles, cobbles and boulders generally trending almost N-S (figure 8). The quartzite occupies less than 5% of the total study area occurring discontinuously along strike. Two textural varieties of quartzite were mapped in the study area; the milky coloured massive and the muscovite-bearing foliated types. Field observations revealed that the rock dips easterly. The N-S trend of the quartzite and its foliation is generally concordant to the trend of schistocity in the neighbouring quartz-mica schist. The micaceous foliation planes as well as the presence of the numerous longitudinal and transverse joints in the rock serve as pathways through which weathering is initiated and accentuated, breaking down the insitu rock into small angular blocks which accounts for why foliated quartzite is rarely found insitu in the study area. Observations on hand specimen shows that the quartzite is essentially composed of over 95 – 100 % quartz with little or no accessory muscovite. Under thin section, quartz occurs mostly in a mosaic of large rectangular sheets of subhedral crystals of various sizes with smoothly interlocking edges, showing strain shadows and undulose extinction (figure 9). Micro-joints in some tabular quartz are healed with recrystallized quartz. Muscovite is slightly pleochroic and occurs as aligned interstitial flakes.

3.3 Quartz-Mica Schist

The schist mapped in the study area is a dark greyish coloured, thinly foliated rock with well-developed millimetric schistose foliations constituted by alternating psammitic and pelitic bands which makes the rock to show tendency to split along preferred plane (figure 10). The former is consistently thicker than the latter. The quartz-mica schist outcrops as discrete concordant body inter-banding with psammitic bands in some parts of the major quartzite bodies in the study area. Good exposures of this rock unit are rare and observed mainly along some major rivers and streams in the area. The rock generally exhibits distinct schistocity with sheen due to the abundance of micaceous minerals in the rock. The quartz mica schist appear to have the highest susceptibility to weathering amongst the rocks mapped in the area and it is therefore commonly found as lowlands and its bare rock exposures are rare. Under thin section (figure 11), the quartz-mica schist is composed of fine flaky muscovite, biotite and hornblende distributed within a matrix of abundant quartz and varying amounts of feldspars. The rock consists of quartz + biotite + orthoclase + andesine + hornblende + muscovite $\pm$ chlorite $\pm$ myrmeckite $\pm$ epidote $\pm$ zircon $\pm$ titanite $\pm$ ore minerals. Muscovite and biotite account for about 20% of the modal composition of minerals in the mica schist.

3.4 Talc Schist

The greyish green coloured rock outcrops either as insitu boulders (figure 12) or as low ridges around the main auriferous quartz vein in the study area. The coarse-grained granular rock which is largely un-metamorphosed, feels soapy to touch. The schist is believed to have been formed from the hydrothermal alteration of a peridotitic precursor which resulted from the considerably varied alteration and replacement products of its constituent minerals particularly biotite and amphiboles. On a tributary to river Weru around the main gold-bearing quartz

vein in the study area, a band of the talcose rock trending 176^{o} with an easterly dip of about 60^{o} and measuring 10-15m wide was exposed on both sides of the bank of the stream within the foliated quartzite host. Under the thin section (figure 13) the rock comprised talc $\pm$ tremolite $\pm$ actinolite + quartz $\pm$ ore mineral. The talcose rock occurs as a greyish fibrous mass of talc with anhedral crystals which forms the groundmass to the phenocrysts of pinkish brown actinolite and greyish green tremolite crystals. Ore minerals occur as isolated anhedral mafic crystals sparsely disseminated within the rock.

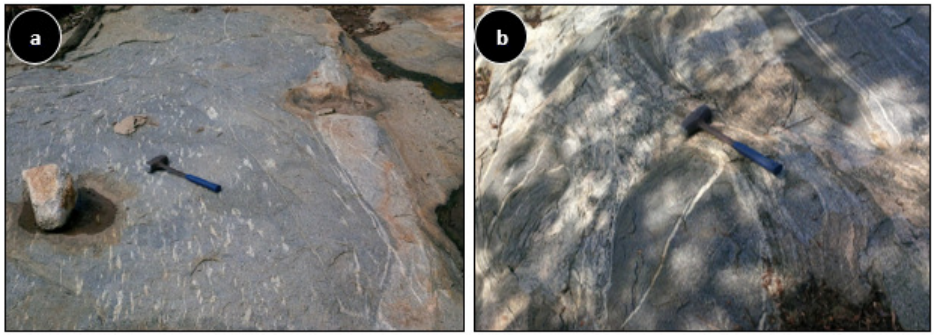


Figure 4: A section of an outcrop of migmatitic gneiss showing (a) ophthalmic (b) schollen structure.

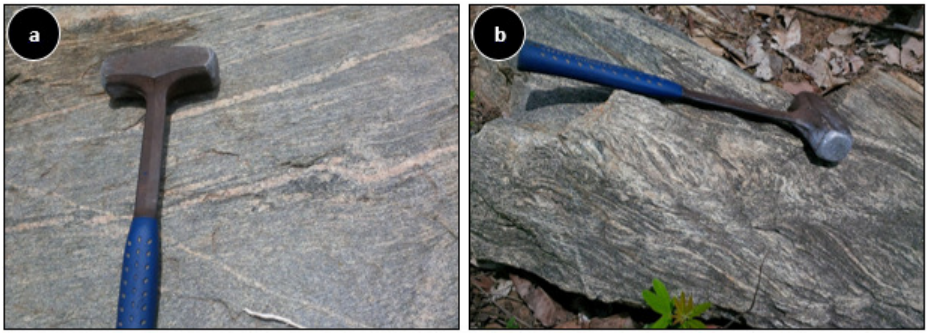


Figure 5: A section of an outcrop of (a) migmatitic gneiss showing stromatic structure, (b) flaggy biotite gneiss.

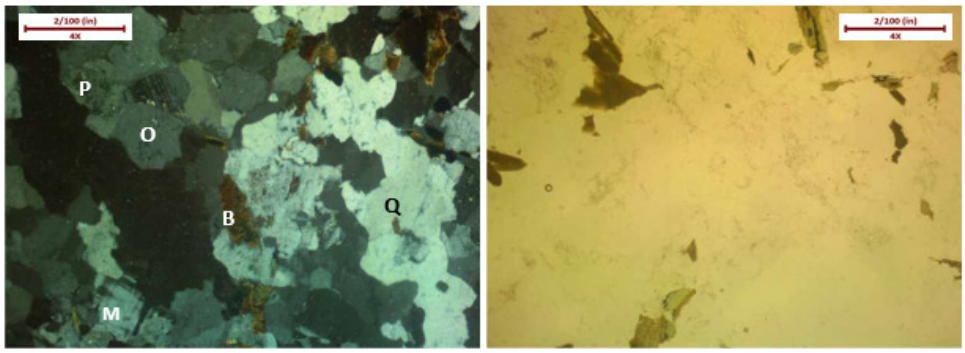


Figure 6: Photomicrograph of granite gneiss in thin section showing (Q= Quartz, P= Plagioclase, O=Orthoclase, M= Microcline and B= Biotite).

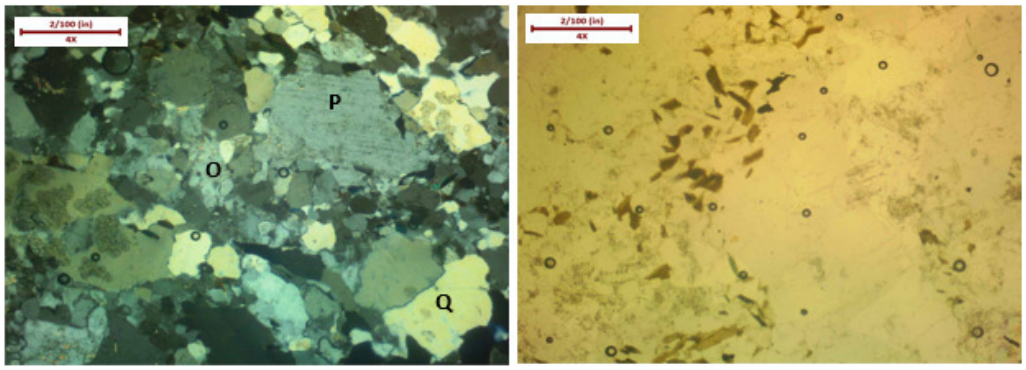


Figure 7: Photomicrograph of augen gneiss under thin section (Q=Quartz, P=Plagioclase and O=Orthoclase).



Figure 8: An outcrop of quartzite showing angular blocks and quartzite rubbles.

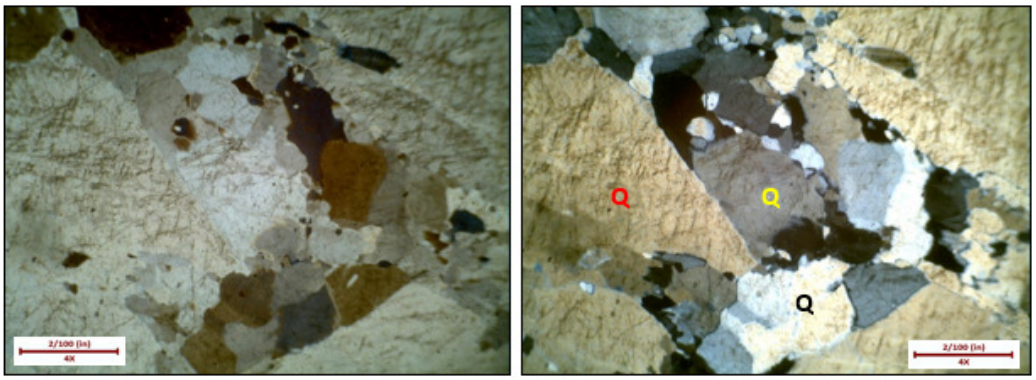


Figure 9: Photomicrograph of the foliated quartzite in thin section under crossed polarized light. Note the micro cross joints in large quartz crystals and the inter-granular spaces healed with recrystallized quartz crystals.



Figure 10: A low-lying outcrop of the quartz-mica schist showing finely foliated schistocity.

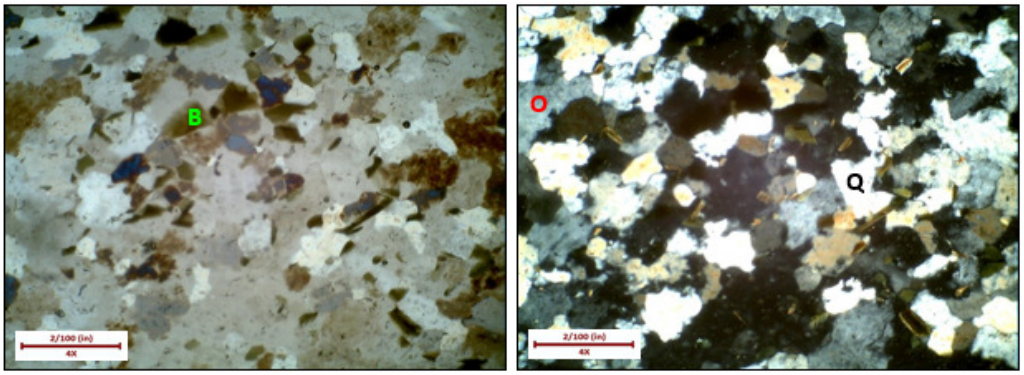


Figure 11: Photomicrograph of the quartz-mica schist in thin section (B=biotite, O=orthoclase, Q=quartz)



Figure 12: An outcrop of the talc-tremolite schist showing insitu boulders.

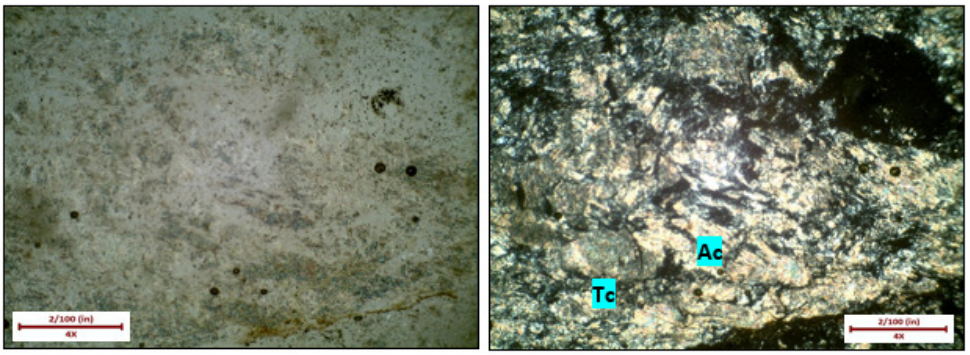


Figure 13: Photomicrograph of the talc-tremolite-actinolite schist in thin section. (Ac=actinolite, Tc=talc)

3.5 Porphyritic Granite

Porphyritic granite underlay about 25% of the study area and outcrops mostly as low ridges in the western and central part of the area. The feldspar megacrysts in the granite generally exhibit a dull chalky luster under weathering condition. The porphyritic granite is coarse grained to porphyritic textured and contain phenocrysts/megacrysts of alkaline feldspar of up to 3cm by 4cm in size within a groundmass of felsic and mafic minerals (figure 14). Thin section studies (figure 15) show that the phenocrysts in the coarse porphyritic granite is composed of microcline and orthoclase within a groundmass of quartz (50%) + plagioclase (15%) + orthoclase (15%) + microcline (10%) + sericite (4%) + biotite (2.5%) $\pm$ hornblende (2%) $\pm$ amphibole (1%) $\pm$ garnet (0.3) $\pm$ ore mineral (0.2%).

3.6 Medium-grained Granite

The rock outcrops as low-lying to low ridge exposures (figure 16) and constitutes about 8% of the mapped area, occurring in the northeastern sector of the area. The medium-grained biotite-hornblende granite is massive, equigranular textured and mesocratic to melanocratic in colour due to abundance of biotite and hornblende. The rock exhibits a sharp contact with the migmatitic gneiss with which it frequently outcrops. Under the thin section (figure 17), the medium-grained granite contains quartz (60%) + orthoclase (15%) + plagioclase (10%) + biotite (8%) + microcline (6%) $\pm$ muscovite (1%). In some slides, few muscovite crystals occur at the grain boundaries of the plagioclase and biotite. The plagioclase is observed being eaten up by orthoclase. Hornblende and biotite are the main mafic minerals in the slide. Some small biotite crystals are poikilitic in large platy orthoclase crystals.

3.7 Porphyroblastic Granite

The Porphyroblastic Granite outcrops mostly as low bare rock ridges in the southeast part of the Study area and exhibits an inferred contact with the granite gneiss to the east. Elsewhere, porphyroblastic granite outcrops as small exposures within its gneissic host rock. The rock is composed of phenocrysts which have been slightly tectonized into porphyroblasts of feldspars within a ground of largely undeformed quartz, feldspar, biotite and hornblende. The Porphyroblasts are formed mainly by microcline and minor plagioclase, where they range in sizes from 1.2cm-4.3cm in length. The porphyroblasts are stretched and aligned in the direction $N38^0E$. Thin section study (figure 18) shows that the porphyroblastic granite is made up of quartz (62%) + plagioclase feldspar (20%) + microcline (13%) $\pm$ biotite (4%) $\pm$ accessory minerals (1%) in order of increasing abundance. Microcline is the most abundant after quartz and make up to about 25% of the total mineral composition of the rock. Microcline is colourless under PPL and shows no pleochroism and a very low birefringence. It shows both albite and pericline twinings, forming a remarkable cross-hatched grid called “tartan plaids”, which distinguishes it from other feldspars. Quartz which is colourless under PPL, with no pleochroism, low refractive index and birefringence, makes up about 62% of the rock.

3.8 Granodiorite

Granodiorite occurs as minor intrusive bodies particularly restricted within the migmatitic gneiss terrain of the study area. They are found as small discordant intrusions cutting the general trend of fabrics in the host rock. A low lying outcrop of the rock was mapped showing intrusions of quartzo-feldspatic veins (figure 19). The granodiorite is frequently associated with xenoliths of gneissic rock whose long axes are variously disoriented. Boudinaged veins of quartz are found as small concordant lenses within the rock. Thin section study (figure 20) reveals that the granodiorite is composed of quartz + labradorite + andesine + orthoclase + microcline + biotite $\pm$ hornblende $\pm$ sericite $\pm$ muscovite $\pm$ myrmeckite $\pm$ orthopyroxene $\pm$ zircon $\pm$ sphene $\pm$ apatite $\pm$ ore mineral. The

rock is rich in plagioclase feldspar composed of labradorite and andesine with polysynthetic twining. Orthoclase eats up the plagioclase feldspar especially at the edges. Microcline is seen as subhedral crystals with cross hatch twining. Sericite is seen as alteration product in microcline feldspar. Biotite is predominant and occurs in clusters of euhedral crystals with no preferred planar orientation and sometimes shows alteration halos at the edges.

3.9 Alkali Syenite

The syenite found within the study area occurs as lenticular, irregular intrusive bodies and dykes in different parts of the migmatitic gneiss, medium-grained granite and porphyritic granite where the rock occurs as small bosses within the host rocks. In some localities, the syenite is mapped as low-lying bare rock outcrops (figure 21). The leucocratic alkali syenite is a feldspar-rich, fine- to medium-grained massive rock showing weak preferred mineral alignment and a flinty fraction. The rock is equigranular and greyish to creamy white in colour. Hand specimen samples of the syenite mapped in the study area is characterized by small needle-like mafic streaks composed essentially of biotite clots. Parallel arrangements of these mafic streaks give the rock some weak sense of mineral alignment. The presence of biotite clusters produces some tiny flakes of biotite when a weathered surface of the rock is scratched with fingernail due to the abundance of the mineral. Field relationship, such as its occurrence as discordant intrusions, shows that the syenite post-dates its gneissic and other granitic hosts. The interlocking relationship between quartz and feldspar gives the rock a granoblastic texture in thin section. Thin section study (figure 22) shows that the rock is composed of quartz + orthoclase + andesine + microcline + biotite + hornblende + muscovite + ore mineral ± bytownite $\pm$ sericite $\pm$ zircon ± allanite ± sphene ± myrmeckite. Quartz is subhedral with triple junction. Plagioclase is andesine with 50% anorthite content.

3.10 Pegmatite and Aplite

Pegmatite and aplite intrude virtually all the basement rock types in the study area, outcropping mostly as minor discordant veins which when locally numerous may coalesce to form large pegmatite bodies. They outcrop mostly as veinlets of a few centimeters wide and are mainly the muscovite bearing, biotite-free type, which frequently host Nb-Ta-Sn minerals within the Nigerian Basement Complex. Two generations of pegmatites have been recognized based on structure and extent of deformation in the study area. Early pegmatites and aplites intruded the gneisses as well as the metasediments while the late stage (post granite) pegmatites and aplites intruded all the rock types in the study area and are relatively undeformed (figures 19 and 23). Thin section observations (figure 24) show that the pegmatites and aplites consist quartz + plagioclase + orthoclase + microcline.

3.11 Vein Quartz

Large volumes of quartz veins outcrop around the central part of the study area, trending discontinuously towards the northeastern sector of the area. Other minor discrete irregular bands, lenses and veins of concordant or discordant quartz infusions were mapped cutting rocks of granites, gneisses as well as the pegmatites of the study area. They range in thicknesses from about 1cm to few tens of meters and trend mostly NE-SW. Most of the quartz veins in the gneisses occur concordantly along the gneissose foliation planes, exhibiting similar trend and dip azimuth as the host rock as observed in figure 25. Discordant quartz veins occur usually along healed joints and fractures in various directions. The concordant quartz veins, from field relationships, appear to have been caught up in tectonism which affected their host rocks while most of the discordant, fracture-filling veins are structureless. Thin section study reveals that the rock is almost entirely composed of anhedral crystals of quartz (98%) $\pm$ muscovite (1.5%) $\pm$ magnetite (0.5%).



Figure 14: An outcrop of coarse porphyritic granite showing sharp contact with biotite-hornblende gneiss.

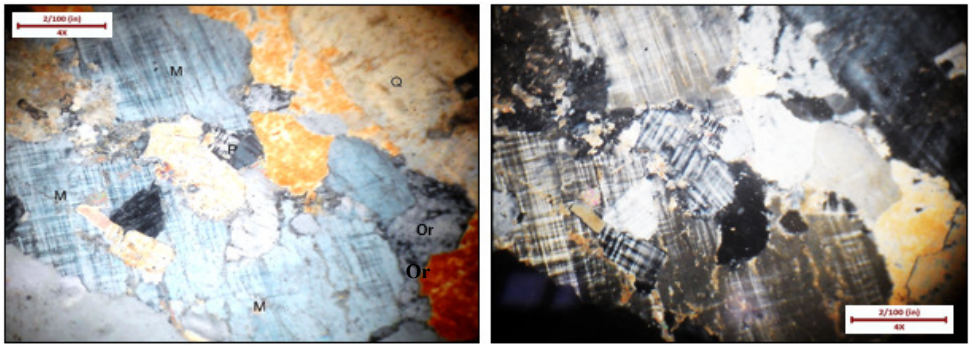


Figure 15: Photomicrograph of the porphyritic granite (M=microcline, P=plagioclase, Or=orthoclase, Q=quartz).



Figure 16: A low ridge outcrop of the medium-grained granite.

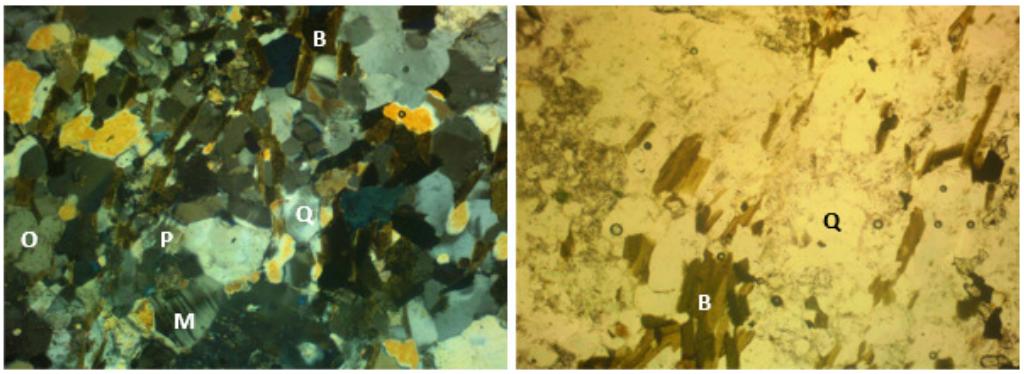


Figure 17: Photomicrograph of medium-grained granite (Q=Quartz, P=Plagioclase, M=microcline, B=Biotite, O=Orthoclase).

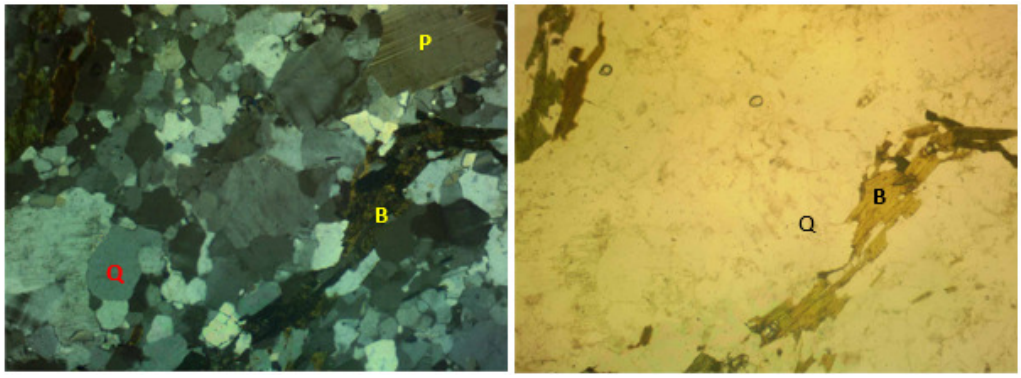


Figure 18: Photomicrograph of porphyroblastic granite (Q= Quartz, B= Biotite and P= Plagioclase).



Figure 19: An outcrop of granodiorite showing pegmatitic intrusion.

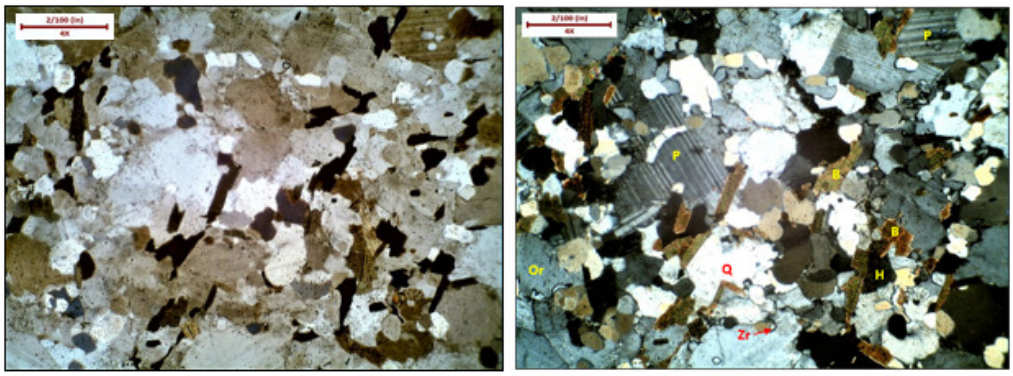


Figure 20: Photomicrograph of the granodiorite (B=biotite, H=hornblende, Or=orthoclase, P=plagioclase, Q=quartz, Zr=zircon).



Figure 21: A low ridge outcrop of the Alkali Syenite.

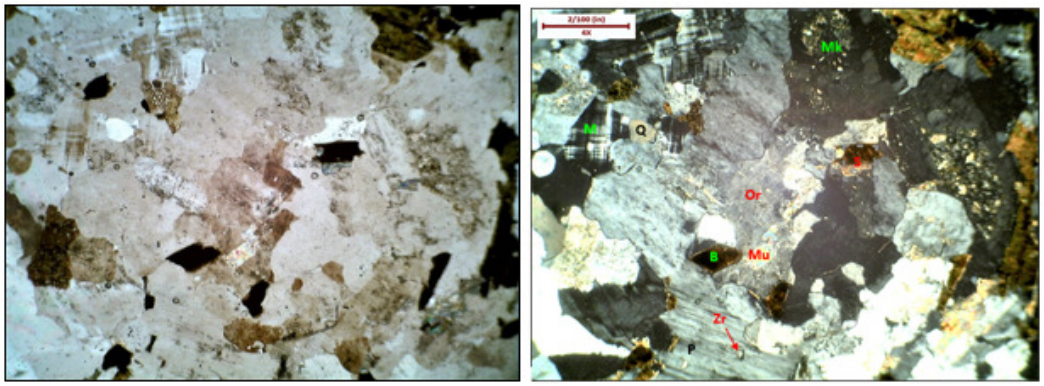


Figure 22: Photomicrograph of alkali syenite (B=biotite, M=microcline, Mk=myrmeckite, Mu=muscovite, Or=orthoclase, P=plagioclase, Q=quartz, S=sericite, Zr=zircon).



Figure 23: An outcrop of medium grained granite showing k-feldspar rich pegmatitic intrusion.

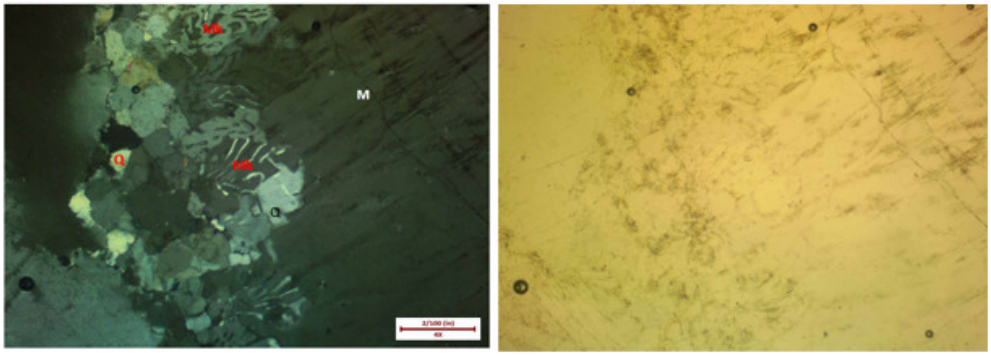


Figure 24: Photomicrograph of quartzo-feldsparthic vein (O=Orthoclase, Q= Quartz, Mk= myrmekite and M= Microcline).



Figure 25: A section of an outcrop of granite gneiss showing a band of concordant quartz vein.

4. Structural Geology

Field observations indicate that the basement rocks have been subjected to many periods of deformation. Several structural elements were mapped within the rocks in the study area. Foliation is the most conspicuous structure in the gneissic terrain where the rock shows folding of the penetrative alignment of alternating dark and light minerals. The strikes of the foliations are mainly in NNE-SSW direction (figure 26a), with an average trend of N34^{0}E which are axial planar to the fold axial trace of tight isoclinal folds. Another very prominent brittle structure is joints which are close or open; healed or unhealed. The joints mapped within the rocks in this area mainly strike in the WNW-ESE direction (figure 26b), where they are mostly observed to cut across the foliation planes. Most of these joints have been healed with vein quartz and pegmatitic intrusions. Major trend of these veins is in the NNE-SSW direction (figure 27a). Several minor folds were mapped in gneissic rocks of the study area whose fold axes are mainly in the NNE-SSW direction (figure 27b).

The average plunge of the fold axes of the tight isoclinal folds (figure 28a) is 15^o to 22^o in the directions 010^o to 045^o and some of the folds are locally recumbent with fold axial planes dipping between 36^o and 60^o either easterly or westerly. Closely related to the tight isoclinal folds are the ptygmatic folds (figure 28b), which are mostly found in the migmatitic gneisses. Another folding episode is expressed as flow structures defining open folds in the gneisses some of whose axial plane are locally recumbent with an average plunge of about 55^o-70^o in the direction 110^o-140^o. On some intensely deformed outcrops, interference between two open folds were observed, resulting in the formation of basin (figure 29a) and dome structure. A major episode of folding is inferred from the set of distinctive bands of gneissosity associated with the gneisses which form excellent structural markers that define regional antiformal and synformal folds whose axes trend almost parallel and NNE-SSW particularly in the southern half of the study area. This episode of folding is perhaps accompanied by semi-brittle deformation that forms the various parallel shears (figure 29b) observed on many gneissic outcrops and may in fact be responsible for tectonizing a section of the porphyritic granite into porphyroblastic granite and gneiss in the area.

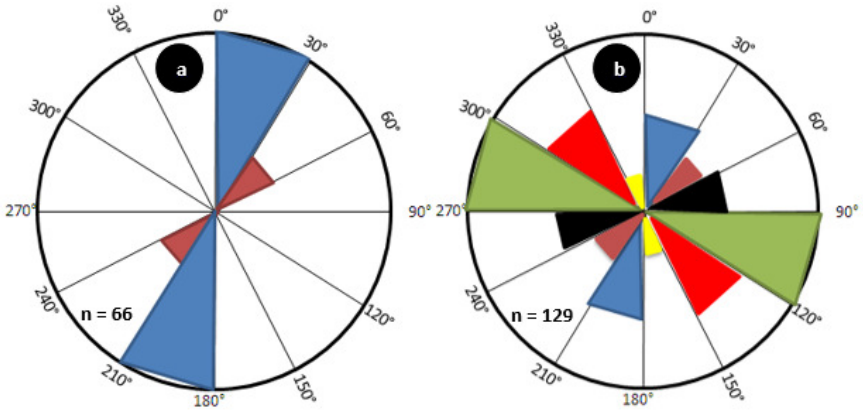


Figure 26: Rosette diagram of (a) strike of foliation plane in gneisses (b) trend of joints direction.

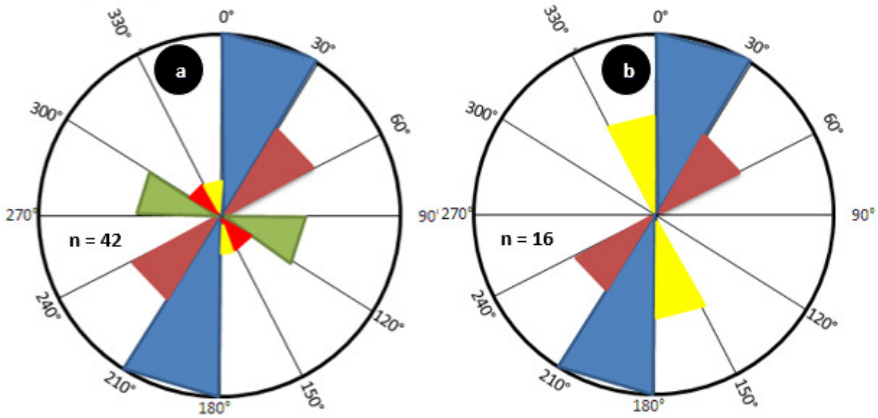


Figure 27: Rosette diagram of trend of (a) quartz veins (b) fold axial traces in the gneisses.

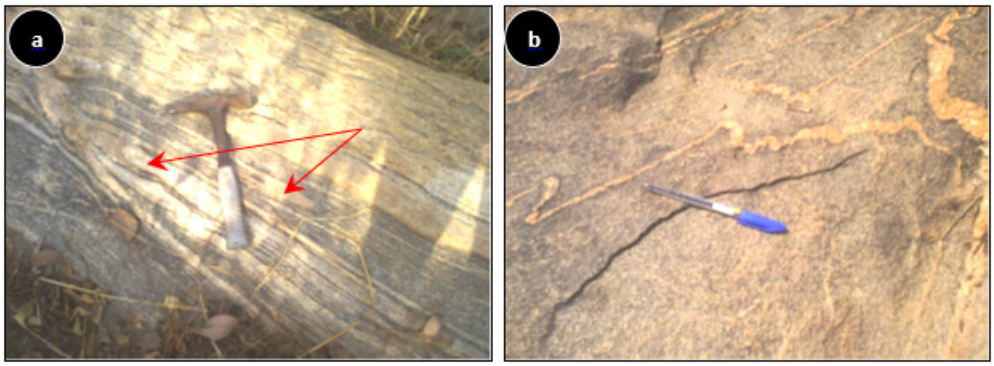


Figure 28: An outcrop of migmatitic gneiss showing (a) tight isoclinal folds (b) ptygmatic folds.

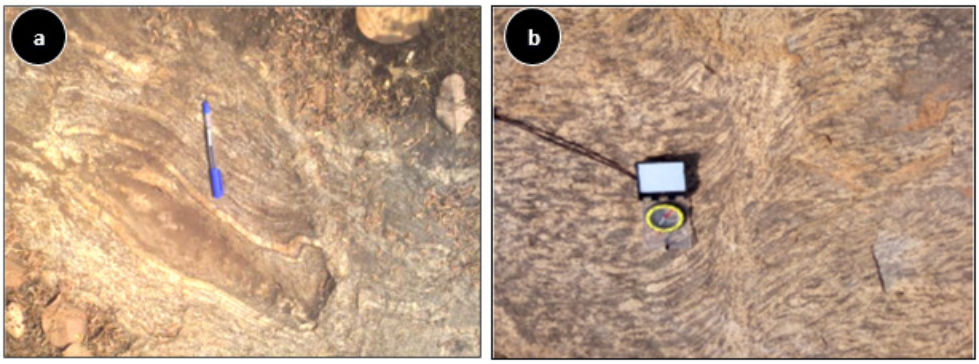


Figure 29: An outcrop of a migmatitic gneiss showing (a) deformed basin structure (b) ductile shear.

4.1 Structural Evolution

The Nigerian basement is polycyclic in nature and it is characterized by different histories of metamorphism, thermo-tectonism and structural modifications (Odeyemi, 1981; Rahaman et al., 1983; Caby, 1989) which are reflected in its complex petrological and structural composition with successive events overprinting, reworking and modifying the earlier events. Field and structural evidence revealed that the basement rocks underlying the study area have suffered multiple episodes of deformations. The gneissic rocks in the area shows structural elements with varying degree of deformation ranging from simple stromatic to intensely deformed contorted foliation planes. The study of the present-day rock geometry with respect to the three-dimensional distribution of the various lithological units provided information about the history of deformation (strain) in the rocks, and ultimately, the stress field that resulted in the observed strain and geometries. Field and petrological evidence suggest at least three episodes of deformation in the study area. The structural deformation (D_1) in the area probably constitute the first tectonic episode which changed the physico-chemical structure of the sedimentary precursor leading to primary metamorphic fabrics that are observed as lithological and mineralogical banding (S_oS_1) preserved in some biotite gneisses located in tectonic shadows. The second tectonic deformation episode (D_2) was responsible for folding the S_oS_1 surfaces into tight isoclinal folds (F_1) which produced the S_2 surfaces that are axial planar to F_1 as observed in figure 28. The third episode of tectonic deformation (D_3) refolded the S_2 surfaces resulting in the formation of the crenulation cleavages which formed the incipient (S_3) surfaces that are superimposed on S_2 surfaces in tectonic shadows on some outcrops. This produce the second filial generation of major folds (F_2), which are upright, open or close and may sometimes be recumbent and plunging. The tectonic features produced by D_3 include pinch and swell structure, similar, asymmetric and chevron folds. D_3 is also perhaps responsible for the formation of the inferred regional folds in the study area and may have resulted in the formation of several regional fractures, minor joints, shears, faults as well as basin and dome structure which may have been produced by the interference between two fold patterns.

5. Gold Exploration in Alagbede Area

5.1 Soil Sampling, Rock Crushing and Panning

In the course of geochemical survey, soil and rock samples were collected around the mineralized vein quartz using appropriate sample collection techniques. A total of 32 soil samples were collected randomly from the three main layers identified as the topsoil 'A' horizon, middle 'B' horizon and saprolitic 'C' horizon at depths mostly ranging from 0.4 to 1m, with the aid of a hand auger, depending on the thickness of the overburden on the underlying basement rocks. Visual observation of samples from all the three horizons in the trench shows visible specks of gold which were observed particularly within the saprolitic horizon. The soil samples were homogenized by mixing and panning produced an average of 0.4g of gold in 50kg of regolith soil samples particularly collected from the prophyllitic zone of the quartzite, syeno-granite and talc schist. For rock sampling, grab samples were collected from fresh surfaces of exposed rock outcrops in abandoned trenches and pits (figure 30) dug previously by artisanal miners to explore for gold on the gold-bearing quartz vein measuring about 12 to 35m wide and 400m long around Alagbede village (figure 31). The fresh grab samples were crushed into gravel-sized fractions and pulverized into about 200 micron size to obtain fine fractions which were analyzed for elemental composition to determine gold concentrations in each rock sample.



Figure 30: An artisanal exploratory pit for mining of gold at Alagbede Gold deposit.

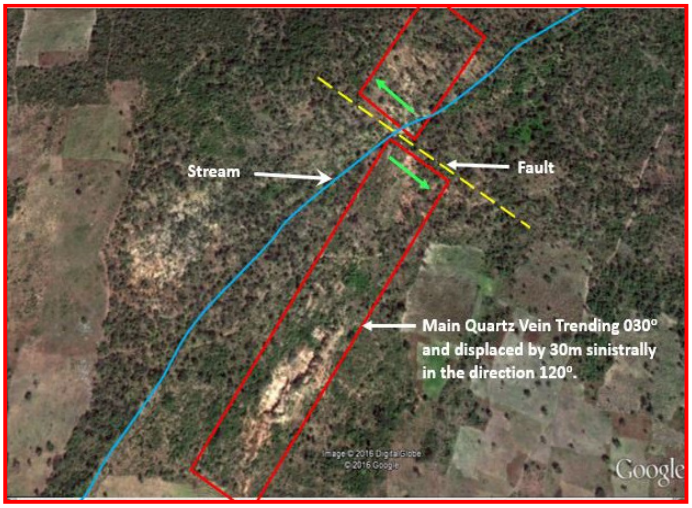


Figure 31: Satellite Image of Alagbede area showing the NE-SW trending mineralized quartz vein.

5.2 Estimation of Ore Grade

A total of 42 rock samples were analyzed, out of which 17 rock samples presented in table 1 indicated appreciable enrichment in gold based on a general background concentration of below 3 ppb of gold for whole rock and stream sediment samples in the study area. Table 1 below shows that gold prospectivity in Alagbede area, from cursory panning of residual soil samples and from fire assay results of rock samples is promising with average gold enrichment values which varies from rock to rock. The result of geochemical analysis of rock samples from the area indicates that lithologies such as quartzite, granites, gabbro and talc schist are enriched in primary gold ranging from an average of 0.24 oz/ton in residual soils, 0.62 oz/ton in gabbro which occur as minor lenses within the gneisses, 0.82 oz/ton in porphyritic granite, 8.12 oz/ton in talc schist, 45.9 oz/ton in syeno-granite, 2.27 oz/ton in low grade vein quartz and 58.64 oz/ton in high grade vein quartz. The low and high grade gold ores in vein quartz have an average combined grade of 23.12 oz/ton.

Table 1: Gold concentration and ore grade in mineralized rocks of Alagbede area.

Sample ID	Fe2O3 %	Cu ppm	Pb ppm	Zn Ppm	Au (ppb)	Au Crustal Enrichment	Au Ore Grade		Av. Ore Grade For Au (Oz/ton)	
							(g/kg)	Oz/ton		
OGp 36	2.32	10.02	12.59	12.1	3.7	1.23	0.0037	0.111	0.822	
OGp 40	2.67	8.154	34.224	53.162	51.1	17.03	0.0511	1.533		
Gab 40B	5.00	8.214	1.892	135.87	17	5.67	0.017	0.510	0.6165	
Gab 52	5.72	31.59	20.82	19.2	24.1	8.03	0.0241	0.723		
VQtz 77	1.46	13.01	7.801	3.275	961	320.33	0.961	28.83	58.64	23.12
VQtz 78	1.41	394.6	3190.2	4589.3	3723	1241	3.723	111.69		
VQtz 80	1.33	23.85	693.22	16	1179.6	393.2	1.1796	35.388		
VQtz 80A	1.52	16.17	3.75	68.7	8.3	2.77	0.0083	0.249	2.27	
VQtz 80C	0.75	7.482	25.198	6.983	82	27.33	0.082	2.46		
VQtz 80D	2.05	6.63	2	39.9	62.7	20.9	0.0627	1.881		
VQtz 80E	0.94	24.38	481.6	11.551	122	40.67	0.122	3.66		
VQtz 81	1.37	40.55	1736.2	25.524	27	9	0.027	0.81		
TSch 79	3.94	4.028	1.115	70.931	662	220.67	0.662	19.86	8.123	
TSch 80A1	12.23	25.65	1.986	190.03	113	37.67	0.113	3.39		
TSch 80B	4.20	42.34	0.788	245.82	217	72.33	0.217	6.51		
TSch 80F	4.14	5.079	1.951	135.07	91	30.33	0.091	2.73		
FAlkGran 85	3.09	59.78	31.437	41.018	4.6	1.53	0.046	45.9	45.9	
Soil samples					-	-	0.008	0.24	0.24	

6. Discussions

Exploration for gold in Alagbede, located in Moro Local Government Area of Kwara State, shows minor gold occurrence in the residual soils around the contact between the quartzite ridge hosting the mineralized vein and the surrounding rocks. These rocks are highly fractured and brecciated with vugs and occasional sulphide mineralization comprising pyrites, chalcopyrite, arsenopyrite and galena which are noticeable in some of the hand specimen. Analytical results of panned concentrates of soil samples from the C-horizon gave an average of 0.4g of gold per 50kg of soil. A higher result of between 1.2 to 2g per 50kg of crushed mineralized vein quartz which is far less than a threshold value of 3.7g/kg of gold obtained from geochemical assay result. These results suggest that Alagbede gold mineralization is not just a show but an hydrothermal economic deposit hosted in the vein quartz that cut through the quartzitic portion of the curvilinear transcrustal fractures which are believed to be linked with gold mineralization in Nigeria. Gold mineralization in Nigeria appears to be the orogenic type which is controlled by deep seated curvilinear transcrustal fracture system. These deep seated fracture systems of Anka-Yauri-Iseyin (AYI) and Kalangai-Zuru-Ifewara (KZI) are believed to serve as conduits to the subsidiary fractures which are linked to these major fractures and form sites of gold deposition.

6.1 Conclusion

A reconnaissance geological investigation of Alagbede area led to the production of a detailed geological map which revealed that the study area is underlain by the basement complex rocks comprising early metamorphic tectonites such as migmatitic gneiss and biotite gneiss on which was deposited the older metasediments including quartzite and talc schist, all of which were intruded by the granitoids and late stage pegmatite and vein quartz in the Pan African time. The evolution and local controls of gold mineralization in the Nigeria Pan African Basement are linked to primary and structural factors. The Pan African thermotectonic Orogeny might have generated heat to establish a thermal gradient for the migration of solutions in veins (Garba, 1993). The concentration of gold in the mineralized vein (VQtz 78) shows a positive correlation with the concentrations of

Cu, Pb and Zn which implies a close association between gold and sulfide ores of chalcopyrite, arsenopyrite, pyrite, galena and sphalerite. Petrology and geochemical assay results revealed that gold occurs as discrete primary ore in rocks such as quartzite, syeno-granite, gabbro and talc schist from where gold ore was leached, remobilized and emplaced in fractures within the gold-sulfide-rich vein quartz by hydrothermal fluids during the Pan African thermotectonic event. The Pan African thermotectonic Orogeny might have generated heat to establish a thermal gradient for the migration of solutions in veins (Garba, 1993). This close association between gold and sulfide ores shows that Alagbede gold deposit occurs initially as small free gold in quartzite, syeno-granite, gabbro and talc schist, and mainly as microfracture-fillings or as inclusions in chalcopyrite, arsenopyrite, pyrite, galena and sphalerite in the vein quartz. This suggest that gold mineralization in the Alagbede is coeval with the precipitation of the sulfide phases which is consistent with the work of Morey et al. (2008) and Large et al. (2009) whose studies have shown that gold is primarily hosted in chalcopyrite, arsenopyrite, pyrrhotite and pyrite in most hydrothermal gold deposits, and that its concentration in sulfide varies to a great extent, and can vary from 0.07 to 1.96 ppm within a single sulfide grain.

References

Caby, R. (1989). Precambrian terranes of Benin-Nigeria and northeast Brazil and the Late Proterozoic south Atlantic fit. Geol. Soc. Am., Spec. Pap., 230, 145-158.

Dustan, W. R. (1911): Reports on the results of the mineral survey of Northern Nigeria, 1907-8 and 1908-9. Colon. Rep. misc. Ser., #79.

Ferre´, E., Gleizes, G., Caby, R., (2002). Obliquely convergent tectonics and granite emplacement in the Trans-Saharan belt of Eastern Nigeria: a synthesis. Precambrian Research 114, 119–219.

Garba, I. (1993): The Geology, Geochemistry and Origin of Gold Mineralization in Bin Yauri, Nigeria. Dept. of Geology, Imperial College PhD thesis.

Geological mapping on Scale 1:50,000 Sheet 224 (Osi N.E, S.E, N.W and S.W), Kwara State, North Central Nigeria.

Garba, I., (2000). Origin of Pan-African mesothermal gold mineralization at Bin Yauri, Nigeria. Journal of African Earth Sciences 31 (2), 433–449.

Garba, I., (2003). Geochemical characteristics of mesothermal gold mineralization in the Pan-African (600 ± 150 Ma) basement of Nigeria. Applied Earth Science (Transaction of the Institution of Mining and Metallurgy, Section B) 112, 319–325.

Grant, N.K., Hickman, M., Burkholder, F.R., Powell, J.L., (1972). Kibaran metamorphic belt in the Pan-African domain of West Africa. Nature (Physical Sciences) 238, 90–91.

GSN (1994). The Schist belts of Nigeria: a publication of the Geological Survey of Nigeria

Large, R. R., Ranyushevsky, L., Hollit, C., Maslennikov, V., Meffre, S., Gilbert, S., Bull, S., Scott, R., Emsbo, P., Thomas, H., Singh, B., and Foster, J. (2009). Gold and trace element zonation in pyrite using a laser imaging technique: Implications for the timing of gold in orogenic and Carlin-style sediment-hosted deposits: Economic Geology and the Bulletin of the Society of Economic Geologists, V. 104, 635-668.

Morey, A. A., Tomkins A. G., Bierlein, F. P., Weinberg, R. F. Davidson, G. J. (2008). Bimodal distribution of gold in pyrite and arsenopyrite. Examples from the Archean Boorara and Bardoc shear systems, Yilgarn craton, Western Australia. Econ. Geol., 103, 599-614.

Odeyemi, I., 1981. A review of the orogenic events in the Precambrian basement of Nigeria, West Africa. Geologische Rundschau, 70: 897-909.

Rahaman, M. A., Emofureta, W. O. and Cean Vacheta, M. (1983). The Potassic of the granites of the Igbetti area: Further Evidence of the Polycyclic Evolution of the pan-Africa Belt in Southwestern Nigeria, Proc. Res. 22, 25-92.

Turner, D.C., (1983). Upper Proterozoic schist belts in the Nigerian sector of the Pan-African province of West Africa. Precambrian Research 21, 55–79.

Woakes, M. and Bafor, B.E. (1984). Primary gold mineralization in Nigeria. Foster (Ed.), In gold '82: The geology, geochemistry and genesis of gold deposits, Geology Soc. Zambia Spec. Pub. (1984), 666-671.

Wright, J.B., Hastings, D.A., Jones, W.B., Williams, H.R., (1985). Geology and Mineral Resources of West Africa. Allen and Unwin, London, 187p.